

# PERFORMANCE OF CODED MFSK IN A RICIAN FADING CHANNEL\*

J.W. MODESTINO AND S.Y. MUI  
Electrical & Systems Eng. Dept., R.P.I.  
Troy, N.Y.

**Summary.** The performance of convolutional codes in conjunction with noncoherent multiple frequency shift-keyed (MFSK) modulation and Viterbi maximum likelihood decoding on a Rician fading channel is examined in detail. While the primary motivation underlying this work has been concerned with system performance on the planetary entry channel, it is expected that the results are of considerably wider interest. Particular attention is given to modeling the channel in terms of a few meaningful parameters which can be correlated closely with the results of theoretical propagation studies. Fairly general upper bounds on bit error probability performance in the presence of fading are derived and compared with simulation results using both unquantized and quantized receiver outputs. The effects of receiver quantization and channel memory are investigated and it is concluded that the coded noncoherent MFSK system offers an attractive alternative to coherent BPSK in providing reliable low data rate communications in fading channels typical of planetary entry missions.

**Introduction.** The use of convolutional codes in conjunction with coherent binary phase-shift-keyed (BPSK) modulation has proven to be an effective and efficient means of obtaining error control on the classical deep space channel. Here the net effect of the channel is simply the introduction of an additive white Gaussian noise (AWGN) component. Recent work by Heller and Jacobs [1] has discussed the performance of short constraint length convolutional codes in conjunction with coherent BPSK modulation and Viterbi maximum likelihood decoding on the AWGN channel while previous work by Jacobs [2] has treated the performance of longer constraint length codes using sequential decoding. In future planetary entry missions, however, the AWGN channel provides an inappropriate model of the propagation environment experienced by an entry probe in transmitting an RF signal at S-Band through a planetary atmosphere. Here it is expected that the signal will undergo fading due to a number of causes including: entry probe dynamics; multipath reflections; and turbulent atmospheric scattering of the RF signal within the planetary atmosphere. Furthermore, because of the typically low data rates associated with planetary entry missions, the oscillator instabilities can be commensurate with the data rate resulting in severe degradation of tracking loop performance with

---

\* This work was supported in part by NASA under contract NGR33-018-188.

subsequent degradation of coherent BPSK system performance. As a result attention has recently been given [3], [4] to noncoherent signaling schemes which are less sensitive to the effects of oscillator instabilities and hopefully perform well in fading channel environments.

In this paper we will describe the implementation and performance of a noncoherent multiple frequency shift-keyed (MFSK) system employing convolutional encoding and Viterbi maximum likelihood decoding. Careful consideration is given to the modeling of the channel in terms of a few meaningful parameters which can be correlated closely with theoretical propagation studies. Primary interest is in the resulting bit error probability performance as a function of  $E_b/N_0$  parameterized by the fading channel parameters, the signaling alphabet size, and the receiver quantization characteristics. While the primary motivation is related to system performance on the planetary entry channel, it is expected that the results are of much wider interest.

**Preliminaries.** A block diagram of the pertinent aspects of the MFSK data link under consideration is illustrated in Figure 1. Here the binary data stream  $\{a_i\}$  is applied as input to a binary convolutional encoder of rate  $R=b/n$ . The binary output digits are grouped into blocks of  $\mu$  digits apiece to produce the output sequence  $\{x_i\}$  where  $x_i \in \{0,1,\dots,M-1\}$  and  $M=2^\mu$  for some specified  $\mu \geq 1$ . The output sequence  $\{x_i\}$  is in turn applied to an MFSK modulator/transmitter producing one of  $M = 2^\mu$  orthogonal tones for subsequent transmission over the channel. The binary convolutional encoder is illustrated in somewhat more detail in Figure 2 where it is assumed that  $n \leq \mu$ . In the remainder of this paper we will consider only the special case  $b=1$ ,  $\mu=n$  so that, in particular, one channel symbol is transmitted for each input information bit.

The encoder output sequence  $\{x_i\}$  applied to the modulator/transmitter produces the channel signaling waveform

$$s(t) = \sqrt{\frac{2E_s}{T_s}} \sum_i \cos(\omega_{x_i} t + \phi_i) p(t-iT_s) \quad (1)$$

where  $p(t)$  is a unit amplitude pulse-like signal of duration  $T_s$  second. The quantity

$$\omega_i = \omega_0 + i\Delta\omega \quad ; \quad i=0,1,\dots,M-1 \quad (2)$$

is the signaling frequency corresponding to the  $i$ 'th tone. Here  $\omega_0$  is some frequency corresponding to the lower bandedge of the transmitted signal spectrum and  $\Delta\omega$  is a fixed frequency increment between adjacent tones. It will be assumed that  $\Delta\omega$  is an integer multiple of  $2\pi/T_s$  so that, in particular, the signaling tones are orthogonal. The sequence  $\{\phi_i\}$  is a sequence of independent and identically distributed (i.i.d.) random variables

uniformly distributed over  $[-\pi, \pi]$ . The independence assumption is obviously required since otherwise the phase could be estimated on the basis of past transmissions violating our assumption of noncoherent reception. The quantity  $E_s$  appearing in (1) is the signal energy per transmitted channel symbol. For the coding scheme under consideration we obviously have  $E_s = E_b$  with  $E_b$  the energy per information bit.

The received signal  $r(t)$  is assumed of the form

$$r(t) = \tilde{s}(t) + n(t) \quad (3)$$

where  $n(t)$  is a zero-mean white Gaussian (WGN) process with double-sided noise spectral density  $N_0/2$  watts/Hz. The received signal component in (3) is then given by

$$\tilde{s}(t) = \sqrt{\frac{2E_b}{T_s}} A(t) \sum_i \cos(\omega_{x_i} t + \phi_i + \theta(t)) p(t - iT_s) \quad (4)$$

where  $A(t)$  and  $\theta(t)$  are respectively amplitude and phase perturbation processes which account for the short-term effects of the transmission medium and/or relative oscillator instabilities between transmitter and receiver. We shall assume that

$$A(t) = |\Gamma + a(t)| \quad (5a)$$

and

$$\theta(t) = \arg[\Gamma + a(t)] \quad (5b)$$

with  $\Gamma = \gamma e^{j\psi}$  a complex quantity whose amplitude  $\gamma$  is fixed and deterministic while the phase  $\psi$  is uniformly distributed over  $[-\pi, \pi]$ . The quantity  $a(t)$  is a complex zero-mean wide-sense stationary Gaussian random process completely described in terms of a channel scattering function  $\sigma(f, \tau)$  as described in [5]. We shall restrict attention to channels dispersive only in frequency with frequency dispersion function of the form

$$\tilde{\sigma}(f) = \frac{\sigma_a^2}{2\pi} \frac{B_0}{B_0^2 + f^2} \quad (6)$$

where  $B_0$  is the coherence bandwidth of the channel in Hz. While other choices are possible, the first order Butterworth spectra represented by (6) provides a reasonable model for a wide variety of channels with memory and at the same time is quite tractable. The resulting autocorrelation function of the  $a(t)$  process in (5) is then given by

$$R_{aa}(\tau) = E\{a(t+\tau)a^*(t)\} = \sigma_a^2 e^{-2\pi B_0 |\tau|} \quad (7)$$

We will assume that the  $a(t)$  process varies slowly relative to an elementary signaling interval of duration  $T_s$  seconds so that it can be considered constant over any such interval

of duration  $T_s$  seconds so that it can be considered constant over any such interval but allowed to vary from interval-to-interval. This is a reasonable assumption for  $B_o T_s \ll 1$ . As a result the signal component in (4) can be expressed as

$$\tilde{s}(t) = \sqrt{\frac{2E_b}{T_s}} \sum_i A_i \cos(\omega_{x_i} t + \phi_i + \theta_i) p(t - iT_s) \quad (8)$$

where  $A_i = |\Gamma + a_i|$ ,  $\theta_i = \arg[\Gamma + a_i]$  and  $a_i$  represents the value of the  $a(t)$  process throughout the  $i$ 'th signaling interval. The sequence  $\{a_i\}$  can be described by the first-order regression

$$a_i = \rho a_{i-1} + W_i; i = 1, 2, \dots, \quad (9)$$

where  $\{w_i\}$  is an i.i.d. sequence of zero-mean complex Gaussian random variates with common variance  $(1-\rho^2)\sigma_a^2$  and  $\rho = \exp\{-2\pi B_o T_s\}$ . For specified values of  $\gamma$  and  $\sigma_a^2$  results can then be determined parametrically as a function of the dimensionless quantity  $B_o T_s$  allowing conclusions to be drawn as a function of the signaling rate  $f_s = 1/T_s$ . The quantity  $B_o T_s$  is of course, indicative of channel memory measured in signaling intervals. Table 1 illustrates typical values of  $B_o$  and  $\sigma_a^2$  for a Venus mission. This data is taken from [6]. The choice  $\gamma=1.0$  is most representative while  $\gamma=0$  is somewhat of a worst case.

L*, km	B <sub>o</sub> , Hz	$\sigma_a^2$	
		$\gamma=0$	$\gamma=1$
55	0.146	1.118	0.112
30	0.112	1.037	0.036
10	0.071	1.005	0.005
5	0.054	1.001	0.001
1	0.029	1.000	

L\* is depth of penetration into Venusian atmosphere

Table 1  
Representative Channel Parameters  
for Venus Mission

During each successive signaling interval the receiver, or alternatively the demodulator detector, illustrated in Figure 1 computes the M statistics

$$z_{mi} = \frac{2}{T_s} \left\{ \int_{(i-1)T_s}^{iT_s} r(t) \cos \omega_m t dt \right\}^2 + \frac{2}{T_s} \left\{ \int_{(i-1)T_s}^{iT_s} r(t) \sin \omega_m t dt \right\}^2 \quad (10)$$

for  $m=0,1,\dots,M-1$ . The actual receiver output is the sequence  $\{r_i\}$  where for each  $i$ ,  $r_i$  consists of the above M components. This will be referred to as the unquantized case. In practice it is desirable to quantize the receiver outputs in some fashion to facilitate

decoding. The particular quantization scheme considered here results in an ordered list of the  $\ell$  largest decision statistics computed during successive signaling intervals. More specifically, in this case  $\underline{r}_i$  is the  $\ell$ -vector.

$$\underline{r}_i = (r_{i_1}, r_{i_2}, \dots, r_{i_\ell}) \quad (11)$$

where  $r_{ij} = m \in \{0, 1, \dots, M-1\}$  provided  $z_{mi}$  is the  $j$ 'th largest statistic  $1 \leq j \leq \ell$  during the  $i$ 'th signaling interval. The case  $\ell=1$  corresponds to the conventional hard decision receiver while if  $\ell > 1$  additional reliability information is provided to the decoder. We refer to this case as list-of- $\ell$  decoding (cf.[7]).

In either case, the decoder performs maximum likelihood decoding of the received vector sequence  $\{\underline{r}_i\}$  making use of the Viterbi algorithm. The appropriate decoding metrics in each case are, of course, different. The details are provided in [8] and will not be repeated here.

**Uncoded System Performance.** In order to evaluate the coding advantage provided by the MFSK system described in the preceding section, it is desirable to provide an evaluation of the uncoded system performance. The symbol error probability in the presence of fading is shown in [8] to be

$$P_e = 1 - \frac{1}{2} \int_0^\infty [1 - \exp\{-\frac{\zeta y}{2}\}]^{M-1} \exp\{-\frac{1}{2}[y + \frac{2\eta E_s}{N_0}]\} I_0[\sqrt{y}(2\eta E_s/N_0)^{1/2}] dy \quad (12)$$

where  $\zeta = 1 + \sigma_a^2 E_s/N_0$  and  $\eta = \gamma^2/\zeta$ . This expression is readily evaluated as a function of  $E_s/N_0$  for fixed values of  $\gamma$  and  $\sigma_a^2$ . Notice that in the absence of fading  $\gamma=1$ ,  $\sigma_a^2=0$  so that  $\zeta=1$  and  $\eta=1$  and (12) reduces to a known result [3],[4].

Of considerably more interest in a comparison with the coded MFSK system is the bit error probability computed from  $P_e$  according to (cf.[ 9])

$$P_b = \frac{2^{n-1}}{2^n - 1} P_e \quad (13)$$

with  $M=2^n$  and the symbol energy  $E_s$  in (12) related to the energy per bit  $E_b$  according to  $E_s = nE_b$ . In future comparisons,  $P_b$  will be computed according to (13) for selected values of  $E_b/N_0$ ,  $\gamma$ ,  $\sigma_a^2$  and  $n$ .

**Bounds on Performance of Coded System.** Recently Viterbi [10] has provided a rather complete analysis binary convolutional codes and their performance in typical communication systems. This work has shown the advantages of the state diagram and generating function approach to analyzing such problem . We will assume some knowledge of this approach and extend it to the analysis of binary convolutional codes

when used in conjunction with M-ary orthogonal signaling alphabets. More specifically, we consider the scheme illustrated in Figure 2 employing a binary rate  $1/n$  code with  $M=2^n$ . As in the binary signaling case we will find that a tight upper bound on the bit error probability can be obtained in terms of the generating function  $T(D,N)$  (cf. [10] for definitions) associated with the particular code employed. For example, a  $K=3$ ,  $R=1/2$  code is used in Figure 3a to generate a 4-ary signaling alphabet while the associated state diagram is illustrated in Figure 3b. A D along any path indicates that the corresponding state transition resulted in the transmission of an M-ary symbol other than the zero symbol. An N along any path indicates that the corresponding state transition was caused by a data "1" shifted into the encoding register. The state diagram differs from that which would have been obtained in the binary signaling case in that the literals D appearing in Figure 3b would then have as exponent the Hamming weight of the corresponding transmitted branch sequence. In the M-ary signaling case we are only concerned with whether or not the state transition resulted in the transmission of the zero channel symbol. As a result the weight(exponent of the literal D) assigned to each branch in the state diagram is at most unity.

The generating function for the code illustrated in Figure 3b is clearly

$$T(D,N) = \frac{D^3N}{1-2ND} = D^3N + 2D^4N^2 + 4D^5N^3 + \dots \quad (14)$$

indicating minimum distance 3 in this new metric. Good codes for this application are those that maximize this minimum distance. It does not follow that good codes for binary signaling (cf. [11], [12]) are necessarily optimum for M-ary signaling as indicated in [8] where a tabulation of good codes for  $K \leq 10$  and  $M=2,4,8,16$  is provided. These codes will be employed in what follows.

Assume the all zero message has been transmitted. We desire to determine the probability of the event that the correct all zero path is rejected for the first time at some level in favor of an incorrect path which differs in exactly k symbol positions. This event is precisely that of choosing incorrectly between two noncoherent orthogonal signals on the basis of a k-fold diversity transmission. Define the k-vectors

$$\underline{A}_k = (A_{k_1}, A_{k_2}, \dots, A_{k_k}) \quad (15a)$$

$$\underline{\theta}_k = (\theta_{k_1}, \theta_{k_2}, \dots, \theta_{k_k}) \quad (15b)$$

where  $A_{k_i}$  and  $\theta_{k_i}$   $i=1,2,\dots,k$  represent respectively the value of the envelope and phase

processes throughout the i'th signaling interval in which the incorrect path differs from the all zero path. The correct all zero path is then rejected in favor of this incorrect path differing in k symbol positions if

$$z_0 \triangleq \sum_{i=1}^k z_{0k_i} < \sum_{i=1}^k z_{m_i k_i} \triangleq z_1 \quad (16)$$

where the sequence  $\{m_i\}$  is completely arbitrary provided it does not include the zero symbol. Clearly  $z_j, j=0,1$  does not depend upon the phase vector  $\underline{\theta}_k$  so that conditioning upon this quantity can be removed. The conditional probability of a first error event given  $\underline{A}_k$  has been shown [8] to be given by

$$P_{E|\underline{A}_k} = \frac{\exp\{-E/N_o\}}{2^k} \frac{1}{\Gamma(k)} \sum_{j=0}^{k-1} \frac{\Gamma(k+j)}{2^j j!} {}_1F_1(k+j; k; \frac{E}{2N_o}) \quad (17)$$

where

$$E = E_b \sum_{i=1}^k A_{k_i}^2 \quad (18)$$

and  ${}_1F_1(m;n;z)$  is the confluent hypergeometric function [13]. It is easily established that for  $k=1$  (17) reduces to

$$P_{E|A_1} = \frac{1}{2} \exp\{-\frac{E}{N_o}\} \quad (19)$$

which is a known result for noncoherent orthogonal signaling.

The following useful bound on the conditional error event probability is provided in [8],

$$P_{E|\underline{A}_k} \leq \left(\frac{e}{4}\right)^{k/2} \exp\{-\frac{E}{4N_o}\} \{1 + 0[(\frac{E}{2N_o})^{-1}]\} \quad (20)$$

which will be used to obtain explicit bounds on the bit error probability  $P_b$ . We will be particularly interested in the case of fast fading where the fading amplitude, although constant within a signaling interval, is independent from interval-to-interval. This can be achieved with sufficiently large interleaving still under the condition  $B_o T_s \ll 1$ . As a consequence, the components of  $\underline{A}_k$  are i.i.d. and after neglecting higher order terms in  $(E/2N_o)^{-1}$  appearing in (20), we have the following bound on the unconditional error event probability.

$$P_E \leq \left(\frac{e}{4}\right)^{k/2} E^k \{ \exp\{-\frac{E_b x}{4N_o}\} \} \quad (21)$$

where  $x$  is a generic random variable which is noncentrally chi-square distributed with two degrees of freedom, variance parameter  $\sigma^2 = \sigma_a^2/2$  and noncentrality parameter  $\gamma^2$ . The expectation appearing on the right-hand side of (21) is easily evaluated in terms of the characteristic function (ch.f.) associated with the random variable  $x$  given by

$$\psi_x(u) = E\{e^{jux}\} = \frac{1}{1-j2u\sigma^2} \exp\left\{-\frac{juy^2}{1-j2u\sigma^2}\right\} \quad (22)$$

In particular, it follows that

$$E\{\exp\{-E_b x/4N_o\}\} = \psi_x(u) \Big|_{u=jE_b/4N_o} \quad (23)$$

so that the first event probability of rejecting the correct all zero path in favor of an incorrect path differing in  $k$  symbol positions is bounded according to

$$P_E \leq \left[ \frac{\sqrt{e}}{2(1+\sigma_a^2 E_b/4N_o)} \exp\left\{-\frac{\gamma^2 E_b/4N_o}{1+\sigma_a^2 E_b/4N_o}\right\} \right]^k \quad (24)$$

Finally, applying the union bound approach of Viterbi [10] we have

$$P_b \leq \frac{dT(D,N)}{dN} \Big|_{N=1, D=D_o} \quad (25)$$

where

$$D_o = \frac{\sqrt{e}}{2(1+\sigma_a^2 E_b/4N_o)} \exp\left\{-\frac{\gamma^2 E_b/4N_o}{1+\sigma_a^2 E_b/4N_o}\right\} \quad (26)$$

This bound is evaluated in Figures 4-5 for  $M=8$  and  $16$  respectively with  $\gamma=1$ ,  $\sigma_a^2=0$  corresponding, of course, to the AWGN channel. The codes in each case were chosen to maximize the weight of the minimum distance path as described previously. In Figure 6 the performance is indicated for  $M=8$  with  $\gamma=1.0$ ,  $\sigma_a^2=0.1$  representing a typical case for a Venus mission according to Table 1. Finally in Figure 7 we illustrate the bit error probability performance as a function of  $E_b/N_o$  for  $M=8$ ,  $K=6$  where now the curves are parameterized by  $\zeta=\gamma^2/\sigma_a^2$  representing the ratio of specular to diffuse energy. The total energy is held constant so that  $\gamma^2+\sigma_a^2=1$  in each case.

**Simulation Results.** Extensive simulation results have been obtained for the coded MFSK system under a variety of channel conditions. Figure 8 illustrates typical behavior for  $M=8$  employing a code with constraint length  $K=6$  and operating on the AWGN channel, i.e., no signal fading present. As indicated, the upper bound does provide a useful asymptotically tight approximation to the operating system performance. Also observe the approximately 0.5 db degradation in system performance over the unquantized receiver using a full list-of- $\ell$  (i.e.,  $\ell=8$  in this case) decoding metric. This is to be expected from consideration of the corresponding union bound parameter  $R_o$  (c.f. [14], Chap. 6). This degradation diminishes to a few tenths of a db for larger  $M$  and a full list decoding metric. The uncoded bit error probability performance is also included in Figure 8 where we observe only a slight coding advantage at typical error probabilities in the range  $10^{-3}$  to  $10^{-4}$ . This advantage does increase in the presence of signal fading.

In Figure 9, the bit error probability performance is illustrated for this same system with  $\gamma=1.0$  and  $\sigma_a^2=0.1$  representing typical channel parameters for a Venus mission. The simulation results correspond to the case of zero channel memory and represent an ultimate performance limit for the chosen values of  $\gamma$  and  $\sigma_a^2$  which can be approached only with sufficiently large interleaving. It is to be noted that the coding advantage can be considerable even for moderate amounts of fading. While the coded system is relatively insensitive to small amounts of signal fading, the uncoded system performance degrades rapidly.

Finally, consider the effects of channel memory. Figure 10 illustrates typical coded system performance for the unquantized receiver parameterized by  $B_oT_s$  under the choice  $\gamma=0$ ,  $\sigma_a^2=1.0$ . This represents a nominal worst case according to Table 1 and the sequel. Observe the rapid degradation in system performance with increasing channel memory (decreasing  $B_oT_s$ ). At high channel signaling rates considerable interleaving would be required to approach the memoryless channel performance. By comparison, a more typical case with  $\gamma=1$ ,  $\sigma_a^2=0.1$  is illustrated in Figure 11. Observe that for moderate amounts of signal fading, the performance is quite insensitive to channel memory. This is in marked contrast to corresponding results for the coherent BPSK system (cf. [4], [15]). The ability to considerably reduce, if not eliminate, interleaving requirements is a considerable advantage of the coded MFSK system for planetary entry missions. Additional simulation results are to be found in [8].

**Summary and Conclusions.** An approach has been presented for the determination and parameterization of the performance of noncoherent MFSK modulation in conjunction with convolutional encoding and Viterbi maximum likelihood decoding on the Rician fading channel. A tight upper bound on bit error probability performance has been presented which can be approached within a few tenths of a db by appropriate receiver quantization and a list-of- $\ell$  decoding metric. The coded MFSK system is shown to provide considerable improvement over the uncoded system in moderate-to-severe fading environments and is relatively insensitive to channel memory. As a result it should prove competitive to coherent BPSK in low data rate planetary entry missions. The error probability performance can be improved considerably with larger constraint length codes in conjunction with sequential decoding strategies. This is a topic of continuing investigation.

## References

1. Heller, J.A. and Jacobs, I.M., "Viterbi Decoding for Satellite and Space Communication", IEEE Trans. Comm. Tech., Vol. COM-19, No.5, Oct. 1971, pp 835-848.
2. Jacobs, I.M., "Sequential Decoding for Efficient Communication from Deep Space", IEEE Trans. Comm. Tech., Vol. COM-15, No. 4, Aug. 1967, pp 492-501.

3. Ferguson, M.J. "Communication at Low Data Rates Spectral Analysis Receivers", IEEE Trans. Comm. Tech. Vol. COM-16, No. 5, Oct. 1968, pp 657-668.
4. Chadwick, H.D. and Springett, J.C., "The Design of a Low Data Rate MFSK Communication System", IEEE Trans. on Comm. Tech., Vol. COM-18, No. 6, December 1970, pp 740-749.
5. Kennedy, R.S., Fading Dispersive Communication Channels, Wiley-Interscience, New York, N. Y. 1969.
6. Modestino, J.W., et.al., "Performance of Convolutional Codes on Fading Channels Typical of Planetary Entry Missions", First Annual Report under NASA Contract NGR 33-018-188, System Engineering Division, Rensselaer Polytechnic Institute, Troy, N. Y. July 1974.
7. Jordan, K.L., "The Performance of Sequential Decoding in Conjunction with Efficient Modulation", IEEE Trans. Comm. Tech., Vol.COM-14, No. 3, June 1960, pp, 283-297.
8. Modestino, J. W., et.al., "Performance of Convolutional Codes on Fading Channels Typical of Planetary Entry Missions", Second Annual Report under NASA Contract NGR 33=018-188, Electrical and Systems Engineering Dept., Rensselaer Polytechnic Institute, Troy, New York, June 1975.
9. Viterbi, A.J., Principles of Coherent Communication, McGraw-Hill Book Co., Inc., New York, N. Y. 1966.
10. Viterbi, A.J., "Convolutional Codes and Their Performance in Communication System", IEEE Trans. Comm. Tech., Vol. COM-19, No. 5, Oct. 1971, pp 750-772.
11. Odenwalder, J.P., "Optimum Decoding of Convolutional Codes", Ph.D. thesis, Syst. Sci. Dept., University of California, Los Angeles, 1970.
12. Larsen, K.J., "Short Convolutional Codes with Maximal Free Distance for Rates  $1/2$ ,  $1/3$ , and  $1/4$ ", IEEE Trans. Inform. Theory, Vol. IT-19, No. 3 May 1973, pp 371-372.
13. Abramowitz, M., and Stegun, I.A., Ed.'s.. Handbook of Mathematical Functions, National Bureau of Standards, Applied Math Series 55.
14. Wozencraft, J.M. and Jacobs, I. M., Principles of Communication Engineering, John Wiley and Sons, Inc., New York, 1965.
15. Modestino, J.W., "Convolutional Code Performance in Fading Channels", Proc. of National Telecommunications Conference, San, Diego, Calif., December 1974, pp, 560-565.

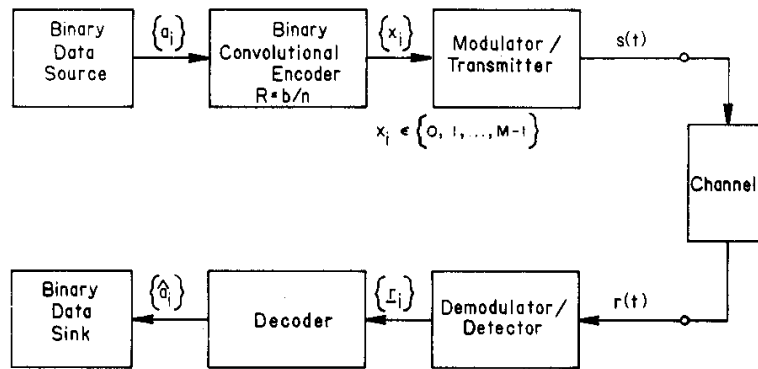


**Figure 1**  
**MFSK System Employing Binary Convolutional Coding**

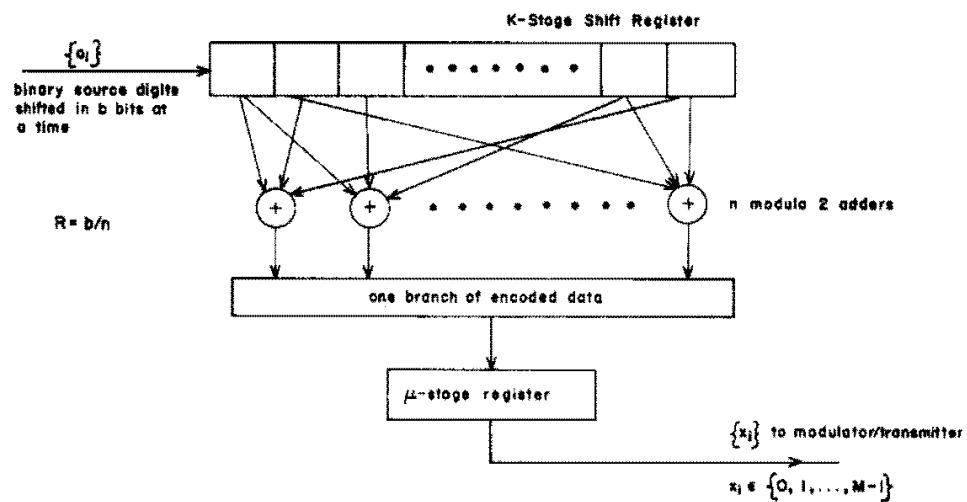
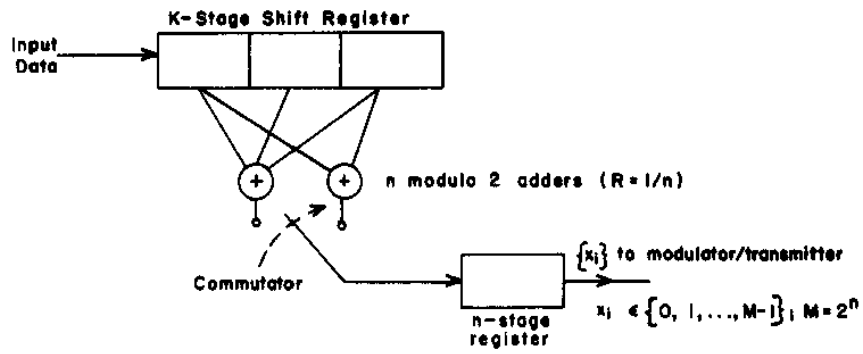
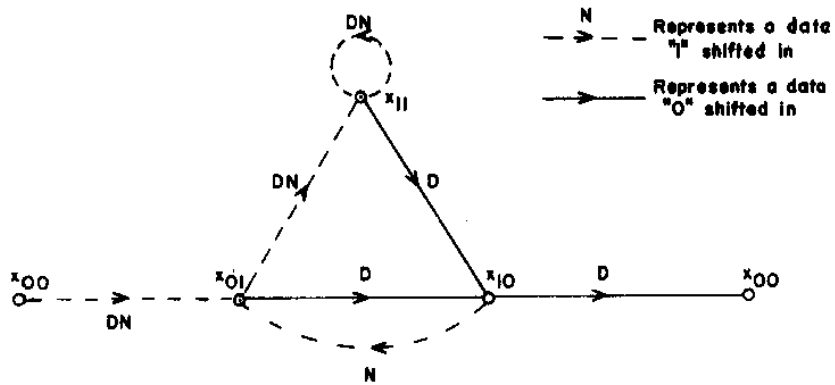


**Figure 2**  
**Use of Binary Convolutional to Implement Coded MFSK System**



a) Convolutional Encoder



b) Corresponding State Diagram

**Figure 3**  
**Typical Convolutional Code Generator and Corresponding**  
**State Diagram for  $K=3, R=1/2$**

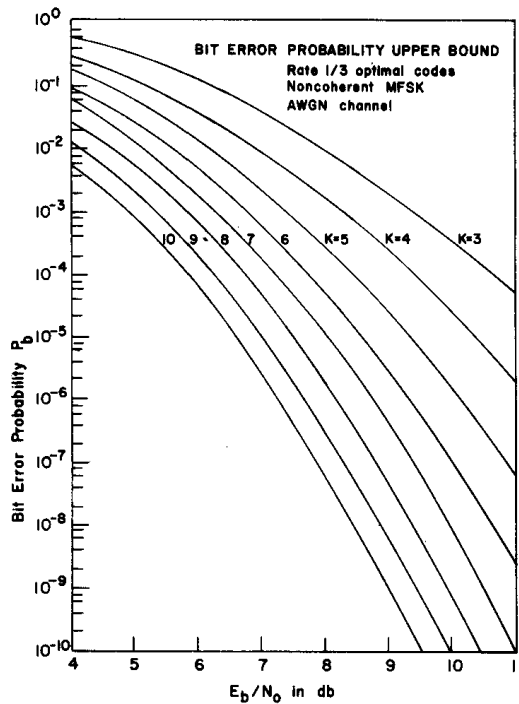


Figure 4

Computed Upper Bound for MFSK System with  $M = 8$  Operating on AWGN Channel

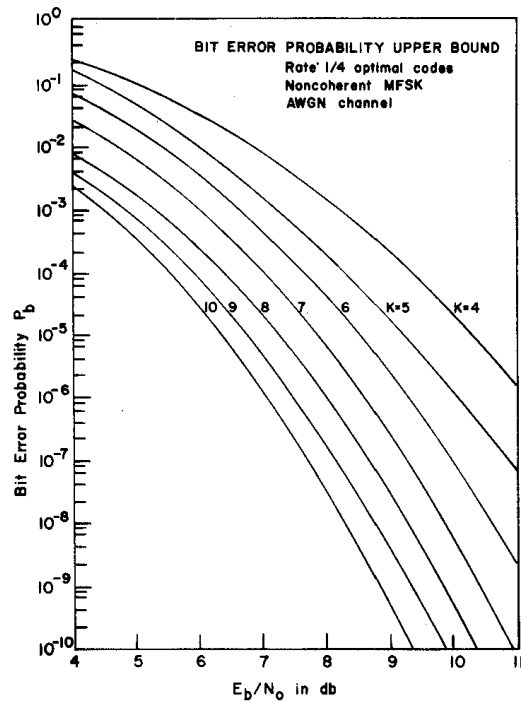


Figure 5

Computed Upper Bound for MFSK System with  $M = 16$  operating on WGN Channel

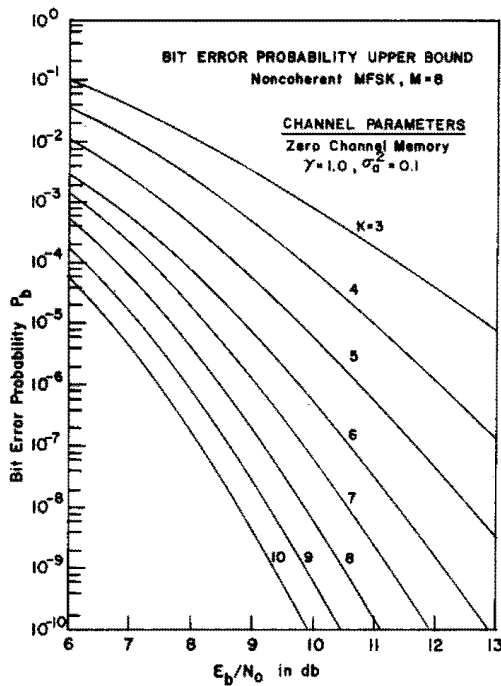


Figure 6

Computed Upper Bound for MFSK System, with  $M = 8$  on Typical Rician Fading Channel

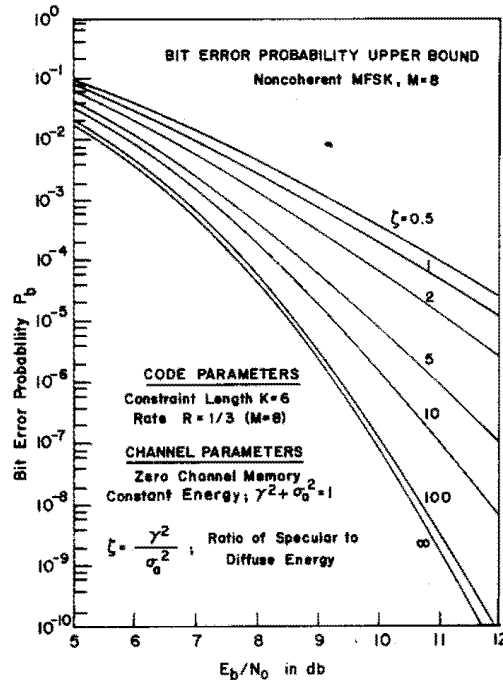
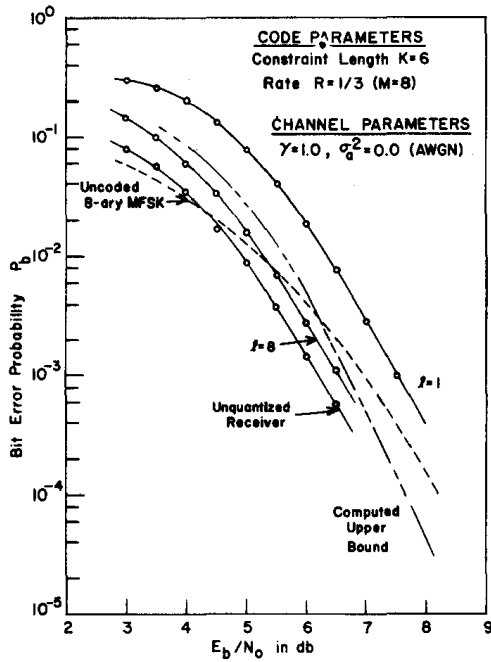
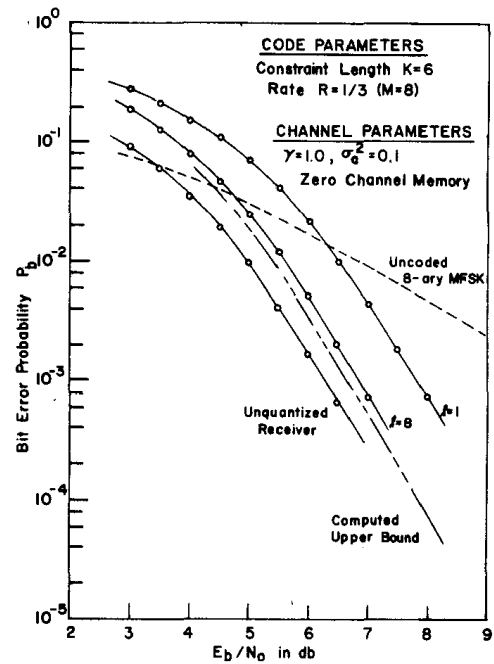


Figure 7

Computed Upper Bound for 8-ary MFSK as Function of the Ratio of Specular to Diffuse Energy



**Figure 8**  
Performance of 8-ary MFSK in  
AWGN Channel



**Figure 9**  
Performance of 8-ary MFSK in  
Typical Rician Fading Channel

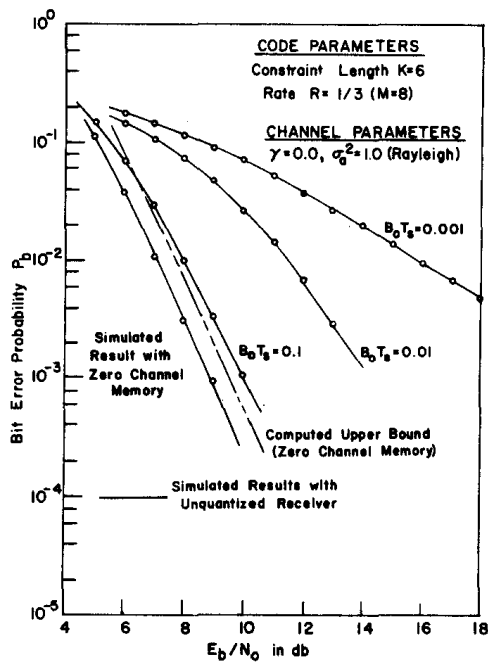


**Figure 10**  
Performance of 8-ary MFSK as a  
Function of Channel Memory  
on Rayleigh Channel

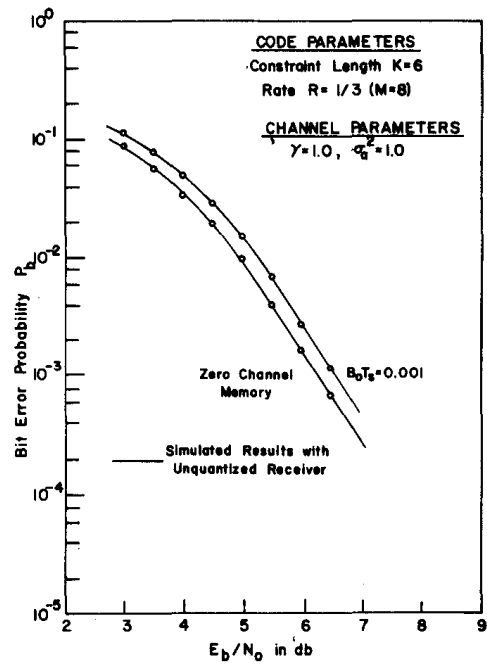


**Figure 11**  
Performance of 8-ary MFSK as a  
Function of Channel Memory on  
More Typical Rician  
Fading Channel